

## Structure–activity relationship and site of binding of polyamine derivatives at the nicotinic acetylcholine receptor

M. Gabriele Bixel<sup>1</sup>, Michael Krauss<sup>1</sup>, Ying Liu<sup>2</sup>, Maria L. Bolognesi<sup>3</sup>, Michela Rosini<sup>3</sup>, Ian S. Mellor<sup>4</sup>, Peter N. R. Usherwood<sup>4</sup>, Carlo Melchiorre<sup>3</sup>, Koji Nakanishi<sup>2</sup> and Ferdinand Hucho<sup>1</sup>

<sup>1</sup>Institut für Biochemie, Freie Universität Berlin, Germany; <sup>2</sup>Department of Chemistry, Columbia University, New York, USA;

<sup>3</sup>Dipartimento di Scienze Farmaceutiche, Università di Bologna, Italy; <sup>4</sup>Department of Life Science, University of Nottingham, UK

Several wasp venoms contain philanthotoxins (PhTXs), natural polyamine amides, which act as noncompetitive inhibitors (NCIs) on the nicotinic acetylcholine receptor (nAChR). Effects of varying the structure of PhTXs and poly(methylene tetramine)s on the binding affinity have been investigated. Using the fluorescent NCI ethidium in a displacement assay  $K_{app}$  values of these compounds have been determined. We found that an increase in size of the PhTX's hydrophobic head group significantly increased the binding affinity, while inserting positive charge almost completely destroyed it. Elongating the PhTX polyamine chain by introducing an additional aminomethylene group decreased the binding affinity, whereas a terminal lysine improved it. In general, poly(methylene tetramine)s showed higher binding affinities than PhTX analogues.

The stoichiometry of PhTX binding was determined to be two PhTX molecules per receptor monomer. PhTXs appeared to bind to a single class of nonallosterically interacting binding sites and bound PhTX was found to be completely displaced by well-characterized luminal NCIs. To elucidate the site of PhTX binding, a photolabile, radioactive PhTX derivative was photocross-linked to the nAChR in its closed channel conformation resulting in labeling yields for the two  $\alpha$  and the  $\beta$ ,  $\gamma$  and  $\delta$  subunits of 10.4, 11.1, 4.0 and 7.4%, respectively.

Based on these findings we suggest that PhTXs and poly(methylene tetramine)s enter the receptor's ionic channel from the extracellular side. The hydrophobic head groups most likely bind to the high-affinity NCI site, while the positively charged polyamine chains presumably interact with the negatively charged selectivity filter located deep in the channel lumen.

**Keywords:** fluorescence titration; nicotinic acetylcholine receptor; noncompetitive inhibitors; photoaffinity labeling; polyamines.

The nAChR belongs to the superfamily of ligand-gated ion channels and is a heteropentameric transmembrane protein with a subunit stoichiometry of  $\alpha_2\beta\gamma\delta$  [1–3]. The five receptor subunits are arranged around a central pore, which is permeable for cations upon agonist binding. The primary structure of each subunit contains four sequences M1–M4 of particular hydrophobicity, which are long enough to traverse the plasma membrane [4]. The M2 sequences from all subunits have been shown to contribute structurally to the formation of the ion pore thereby facing the lumen of the channel [5]. The selectivity filter for cations is formed by several rings of negatively charged amino acid side chains protruding into the lumen of the pore [6–8].

Two well differentiated ligand binding domains are characterized on the nAChR. In the extracellular region the agonist binding sites are located mainly on both  $\alpha$  subunits [1], more precisely at the  $\alpha$ – $\delta$  and  $\alpha$ – $\gamma$  interfaces [9,10]. On the other

hand, several high-affinity binding sites for noncompetitive inhibitors (NCIs), such as triphenylmethylphosphonium (TPMP<sup>+</sup>), have been found within the ion channel on the M2 transmembrane domain [11,12]. Luminal NCIs are assumed to enter the open channel and to bind to different rings within the selectivity filter, thereby inhibiting the ion conductance by sterically plugging the channel pore [13].

The digger wasp *Philantus triangulum*, which preys on honeybees, produces a paralyzing venom with immediate central and peripheral effects. As active ingredients these venoms were found to contain philanthotoxins (PhTXs) [14,15]. These natural polyamine amides of low molecular mass carry positive charges at physiological pH, which should bind to any receptor with a corresponding distribution of anionic functionalities [16]. It is perhaps not surprising therefore that polyamine amides and polyamines interact with cation-selective ion channels such as the nAChR [17–20], ionotropic glutamate receptors [16] and voltage-dependent Ca<sup>2+</sup>-channels [21]. All PhTXs share common structural elements. The head group is formed by a hydrophobic moiety, which is linked to a positively charged tail structure. In initial studies Anis *et al.* [22] and Nakanishi *et al.* [23], for example, demonstrated that the binding affinity can be influenced by altering structural elements of PhTX. Using the radiolabeled channel blocker histrionicotoxin in a displacement test the authors determined IC<sub>50</sub> values of several PhTX derivatives. However,  $K_{app}$  values could not be calculated from their data.

Correspondence to F. Hucho, Institut für Biochemie, Freie Universität Berlin, Thielallee 63, D-14195 Berlin, Germany. Fax: + 49 30 8383753, Tel.: + 49 30 8385545, E-mail: hucho@chemie.fu-berlin.de

Abbreviations:  $\alpha$ -BTX,  $\alpha$ -bungarotoxin;  $K_{app}$ , apparent  $K_d$ ; MALDI, matrix-assisted laser-desorption-ionization; nAChR, nicotinic acetylcholine receptor; NCI, noncompetitive inhibitor; PhTX, philanthotoxin; RP-HPLC, reversed-phase HPLC; TPMP<sup>+</sup>, triphenylmethylphosphonium.

(Received 15 July 1999, revised 25 October 1999, accepted 28 October 1999)

PhTXs are of special interest because potent inhibitors of selectively one type of cation-selective ion channel could be designed from these compounds by chemically altering elements of their structure, which determine receptor specificity and binding affinity. Furthermore, highly active photolabile analogues could be used as powerful tools to explore in photocross-linking studies the three-dimensional structure of the receptor's ligand binding domain.

The aim of the present study was to develop novel, more potent polyamine derivatives, which selectively inhibit the nAChR, by varying the structure of several PhTX and poly(methylene tetramine)s. We investigated the fluorescent NCI ethidium in a titration assay to determine  $K_{app}$  values of these compounds. It was important to utilize an assay other than the previously histronicotoxin displacement test, as this frog toxin is available only in very limited amounts. To determine the stoichiometry of PhTX binding and to further characterize the PhTX ligand binding site, we used a radioactive photolabile PhTX derivative in direct binding assays and in photocross-linking experiments.

## MATERIALS AND METHODS

### Materials

Carbachol, *N*-carbonyloxy-tyrosine-*p*-nitrophenyl ester,  $\alpha,\epsilon$ -bis(*tert*-butoxycarbonyl)-lysine hydroxysuccinimide ester, glutardialdehyde, ethidium and tetracaine were obtained from Sigma (Deisenhofen, Germany). TPMP<sup>+</sup> was from Aldrich (Steinheim, Germany).  $\alpha$ -BTX was from Molecular Probes (Leiden, Netherlands). Na<sup>125</sup>I was purchased from Amersham Buchler (Braunschweig, Germany). Solvents were obtained from Ferosa (Barcelona, Spain). PhTX derivatives were provided from K. Nakanishi (Dept. of Chemistry, Columbia University, New York, USA) and described in detail elsewhere (Nakanishi *et al.* [23]). Poly(methylene tetramine) derivatives were obtained from C. Melchiorre (Dept. of Pharmaceutical Science, University of Bologna, Bologna, Italy).

### Fluorescence titration

All fluorescence spectra were recorded using an Aminco Bowman spectrometer series 2 (Rochester, USA). AChR-rich membranes were prepared from frozen *Torpedo californica* electric organ as described earlier [24]. For fluorescence titration experiments aliquots of competing ligand were added stepwise to a solution containing nAChR-rich membranes (1  $\mu$ M receptor concentration), ethidium (3  $\mu$ M or 6.5  $\mu$ M) and carbachol (1 mM) in 50 mM NaPi, pH 7.4. Ethidium fluorescence was measured by employing an excitation wavelength of 480 nm (slit widths: 4 nm/4 nm) while monitoring the emission from 540 nm to 740 nm. For chemical cross-linking nAChR-rich membranes were incubated with 3  $\mu$ M ethidium and 1 mM carbachol in 50 mM NaPi, pH 8.3. Glutardialdehyde was added yielding a final concentration of 4 mM. After 24 h incubation at room temperature, the cross-linked nAChR was diluted with 50 mM NaPi, pH 7.4 containing 3  $\mu$ M ethidium and 1 mM carbachol to a final

receptor concentration of 1  $\mu$ M and was used for fluorescence measurements.

### Analysis of ligand binding

Dissociation constants ( $K_{app}$  values) for nonfluorescent competing ligands were derived from analysis of their capacity to displace the fluorescent ligand, ethidium. Fluorescence data were plotted according to a logarithmic formula described by Herz *et al.* [25]:

$$\log(f_{EtBr} - f) \cdot \log^{-1}(f - f_{NCI}) = n_H \cdot \log(K_{EtBr}/K_{NCI}) + n_H \cdot \log[EtBr] \cdot \log^{-1}[NCI]$$

$$\text{with } [NCI] = [NCI_0] - ((f_{EtBr} - f)/(f_{EtBr} - f_{NCI})) \cdot [nAChR]$$

$$\text{and } [EtBr] = [EtBr_0] - ((f - f_{NCI})/(f_{EtBr} - f_{NCI})) \cdot [nAChR]$$

where  $f_{EtBr}$  denotes the fluorescence in absence of competing toxins,  $f_{NCI}$  denotes the fluorescence when bound ethidium was completely displaced from the nAChR by TPMP<sup>+</sup> (100  $\mu$ M), and  $f$  denotes the fluorescence observed at any given concentration of competing toxin during the back titration. [NCI] and [EtBr] represent free concentrations of the competing toxin and ethidium, respectively, and  $K_{NCI}$  and  $K_{EtBr}$  their respective dissociation constants ( $K_{EtBr} = 1 \mu$ M; [25]). Hill plots of the competitive dissociation of ethidium from nAChR membranes were calculated from the loss in ethidium fluorescence obtained by the toxins investigated

### Synthesis of N<sub>3</sub>-Ph-PhTX-343-Lys

N<sub>3</sub>-Ph-PhTX-343-Lys was synthesized using a modification of a protocol described previously [26]. *N*-Carbonyloxy-tyrosine-*p*-nitrophenyl ester was coupled with excess spermine in anhydrous tetrahydrofuran at room temperature. The product was purified with silica gel eluting with CH<sub>2</sub>Cl<sub>2</sub>/MeOH/isopropylamine (4 : 4 : 1), and was reacted with  $\alpha,\epsilon$ -bis(*t*-butoxycarbonyl)-lysine hydroxysuccinimide ester in tetrahydrofuran. The resulted adduct was purified with silica gel eluting with CH<sub>2</sub>Cl<sub>2</sub>/MeOH/isopropylamine (80 : 15 : 3). The two secondary amino groups were then protected by di-*t*-butyl dicarbonate in CH<sub>2</sub>Cl<sub>2</sub> and the carbonyloxy group was removed by hydrogenation with palladium on activated carbon (10%) in MeOH, yielding the intermediate NH<sub>2</sub>-PhTX-343-Lys-(Boc)<sub>4</sub>, which was coupled with *p*-azido benzoic acid using 1-(3-dimethylaminopropyl)-3-ethylcarbodiimide hydrochloride, giving N<sub>3</sub>-Ph-PhTX-343-Lys-(Boc)<sub>4</sub>. Deprotection was carried out in trifluoroacetic acid containing 2% thiophenol at room temperature. N<sub>3</sub>-Ph-PhTX-343-Lys was purified by: (a) elution from amberlite OH<sup>-</sup> resin with H<sub>2</sub>O, and (b) elution from triethylamine-saturated silica gel with MeOH containing 0.5% and 10% isopropylamine.

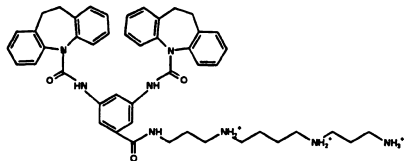
### Synthesis and purification of bi-<sup>125</sup>I-labeled N<sub>3</sub>-Ph-PhTX-343-Lys

N<sub>3</sub>-Ph-PhTX-343-Lys was radioactively iodinated with <sup>125</sup>I using the chloramine T method [27]. The bi-<sup>125</sup>I-derivative was isolated by reversed-phase high-performance liquid chromatography (RP-HPLC) on a Vydac C<sub>18</sub> column applying the

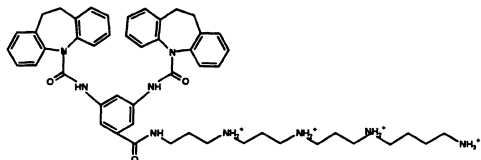
**Fig. 1.** Chemical formulas of the PhTX and poly(methylene tetramine) derivatives tested at the nAChR. The PhTX analogues were derived from the natural toxin PhTX-433, which was shown to have a butyryl/tyrosyl/spermine structure (the numerals indicate the numbers of methylenes between the amine groups of the spermine moiety). The poly(methylene tetramine) analogues share as a common structure a carbon chain, which is separated by four amine groups. The symmetric and asymmetric derivatives were coupled at the end of the polymethylene chain to one and two aromatic groups, respectively. (See following page.)

**A Dihydrocarbamazepine PhTX derivatives**

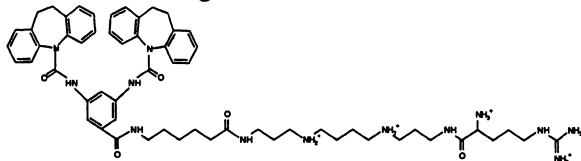
DCB-343



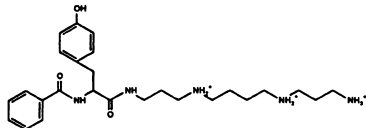
DCB-3334



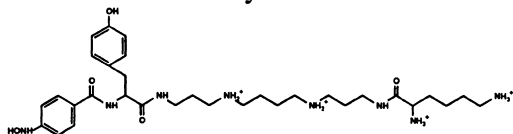
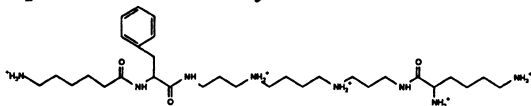
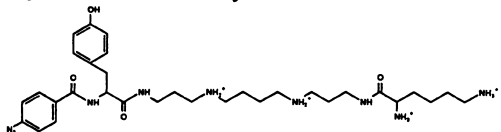
DCB-C6-343-Arg

**C Simple PhTX derivatives**

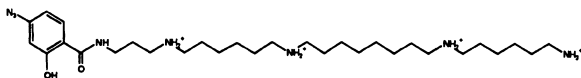
Ph-PhTX-343



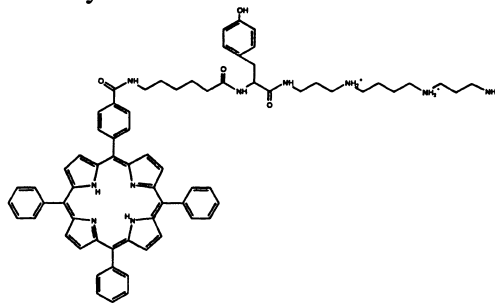
HONH-PhTX-343-Lys

H<sub>2</sub>N-C6-PhTX-343-Lys**D Azido polyamine derivatives**N<sub>3</sub>-Ph-PhTX-343-Lys

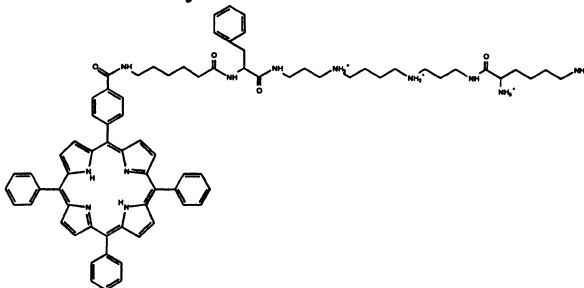
MR44

**B Porphyrin PhTX derivatives**

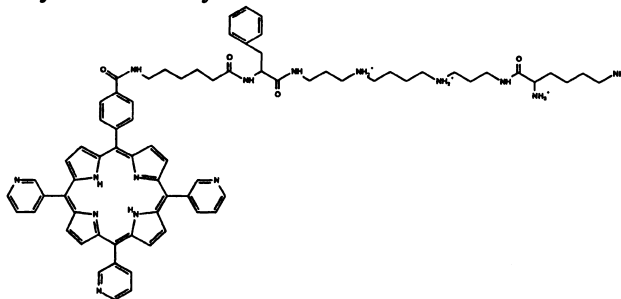
TTP-Tyr-343



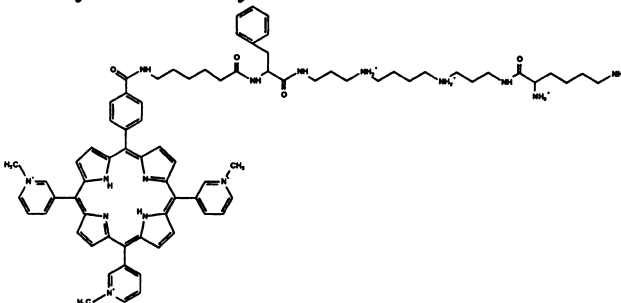
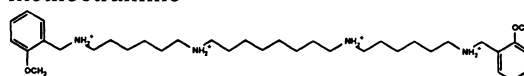
TPP-Phe-343-Lys



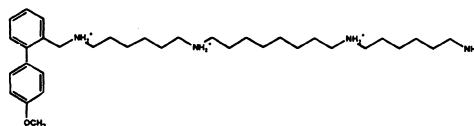
TPyP-Phe-343-Lys



TMePyP-Phe-343-Lys

**E Polymethylene tetramines methoctramine**

MR1996



following linear gradient ( $1 \text{ mL}\cdot\text{min}^{-1}$ ): solvent A (aqueous solution containing 0.1% trifluoroacetic acid) and solvent B (acetonitril containing 0.085% trifluoroacetic acid). The UV-absorption of the HPLC fractions was determined at 280 nm and the radioactivity of each fraction was detected using a  $\gamma$ -counter. The bi- $^{125}\text{I}$ -derivative was characterized by matrix-assisted laser-desorption-ionization (MALDI)-mass spectrometry.

### $\text{N}_3\text{-Ph-}^{125}\text{I}_2\text{-PhTX-343-Lys}$ binding assay

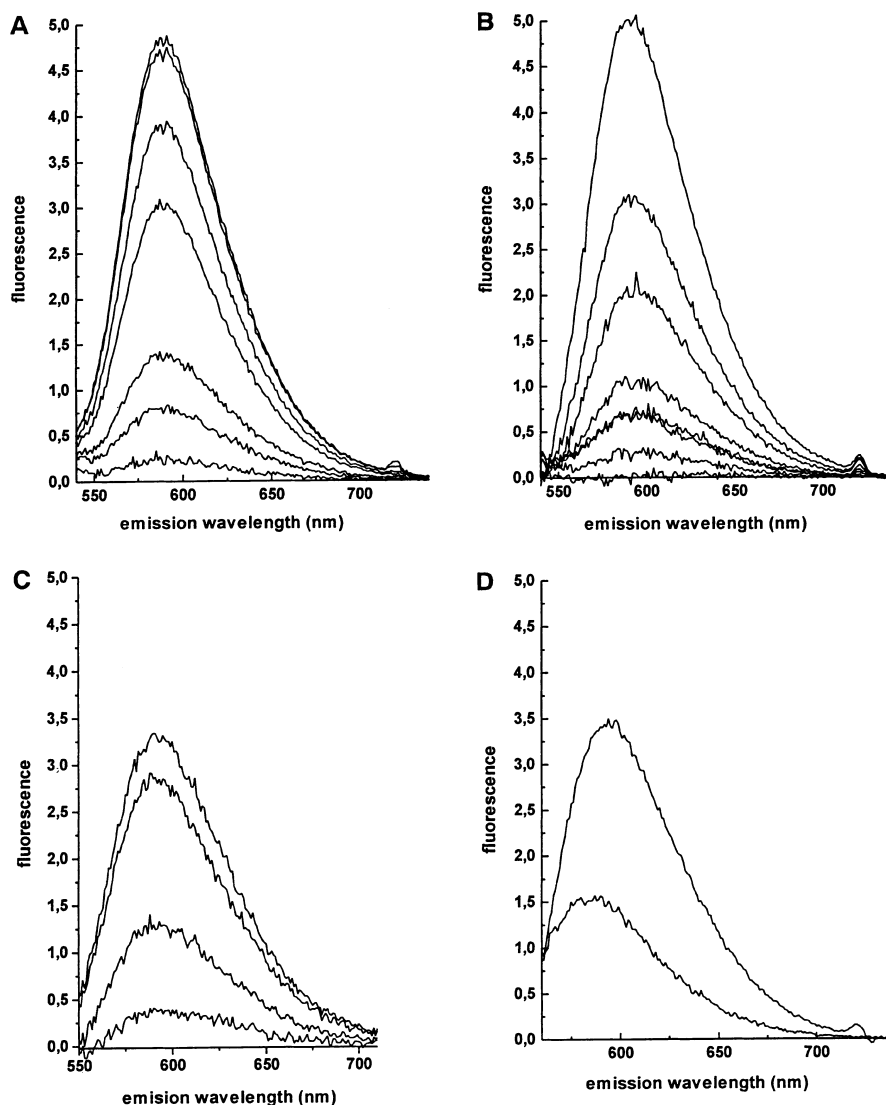
Increasing concentrations of  $\text{N}_3\text{-Ph-}^{125}\text{I}_2\text{-PhTX-343-Lys}$  ( $5000 \text{ c.p.m.}\cdot\text{nmol}^{-1}$ ) were added to a constant amount of nAChR-rich membranes ( $0.3 \text{ mg}\cdot\text{mL}^{-1}$  protein, diluted in  $100 \text{ mM NaPi}$ , pH 7.4; total volume per sample,  $200 \mu\text{L}$ ) and were incubated for 45 min at room temperature. Bound ligand was separated from the free ligand by ultracentrifugation in a Beckmann tabletop ultracentrifuge for 10 min at  $80\,000 \text{ g}$  and  $4^\circ\text{C}$ . Aliquots were withdrawn prior to centrifugation to determine total counts and duplicate aliquots of the supernatant were removed after centrifugation to determine free ligand concentration. Nonspecific binding was determined from bound  $\text{N}_3\text{-Ph-}^{125}\text{I}_2\text{-PhTX-343-Lys}$  in the presence of 100-fold molar

excess of  $\text{N}_3\text{-Ph-}^{125}\text{I}_2\text{-PhTX-343-Lys}$ .  $\alpha\text{-BTX}$  binding assays have been performed as described previously [28].

### Photocross-linking experiments

nAChR-rich membranes were diluted in  $0.1 \text{ M NaPi}$ , pH 7.4 to a final receptor concentration of  $140 \text{ nM}$ . After addition of carbachol ( $500 \mu\text{M}$ ) the samples were incubated for 30 min at room temperature. Subsequently,  $\text{TPMP}^+$ ,  $\alpha\text{-BTX}$  or unlabeled  $\text{N}_3\text{-Ph-PhTX-343-Lys}$  was added and the samples were incubated for further 30 min at room temperature. The radioactive  $\text{N}_3\text{-Ph-}^{125}\text{I}_2\text{-PhTX-343-Lys}$  ( $10 \mu\text{M}$ ;  $250\,000 \text{ c.p.m.}\cdot\text{nmol}^{-1}$ ) was mixed with the sample solution followed by UV-irradiation at  $254 \text{ nm}$  for 45 s. Irradiation times longer than 2 min irreversibly damaged the vast majority of nAChR resulting in high molecular aggregations of the receptor (data not shown). Unbound toxin was separated from  $\text{N}_3\text{-Ph-}^{125}\text{I}_2\text{-PhTX-343-Lys}$  bound to nAChR-rich membranes by centrifugation ( $15\,000 \text{ g}$ , 15 min). The pellet was dissolved and separated by a 10% SDS/PAGE [29]. The stained gel was dried and radioactive receptor subunits were visualized by autoradiography. Cross-linking yields were obtained by slicing the dried gel and measuring the radioactivity of each fraction in

**Fig. 2.** Effect of the NCIs  $\text{TPMP}^+$  and DCB-343 on the fluorescence difference spectra of ethidium bound to nAChR-rich membranes. (A,B) Fluorescence emission difference spectra of nAChR in the presence of  $1 \text{ mM}$  carbachol and  $3 \mu\text{M}$  ethidium with increasing concentrations of  $\text{TPMP}^+$  (A:  $100 \text{ nM}$ – $100 \mu\text{M}$   $\text{TPMP}^+$ ) or increasing concentrations of DCB-343 (B:  $100 \text{ nM}$ – $100 \mu\text{M}$  DCB-343;  $100 \mu\text{M}$   $\text{TPMP}^+$ ). (C,D) Effects of  $\text{TPMP}^+$  (C) and DCB-343 (D) on the fluorescence spectrum of nAChR, which was covalently cross-linked with glutaraldehyde to abolish allosteric mechanisms. Fluorescence difference spectra of cross-linked nAChR in presence of  $1 \text{ mM}$  carbachol and  $3 \mu\text{M}$  ethidium with increasing concentrations of  $\text{TPMP}^+$  (C: 1, 10, 35,  $85 \mu\text{M}$   $\text{TPMP}^+$ ) or with DCB-343 [D:  $75 \mu\text{M}$  DCB-343 ( $\text{IC}_{50}$  value);  $100 \mu\text{M}$   $\text{TPMP}^+$ ]. The nAChR concentration was  $1.3 \mu\text{M}$ . The excitation wavelength was  $480 \text{ nm}$  and the emission was measured at  $590 \text{ nm}$ . Difference spectra were obtained by subtracting the fluorescence spectra determined with increasing concentration of NCI from the spectra measured in absence of NCI.



a  $\gamma$ -counter. The labeling yields were calculated in percentage of mol cross-linked PhTX per mol nAChR subunit.

## RESULTS

To determine binding affinities of various NCIs at the high affinity NCI site of the nAChR a displacement assay using the fluorescent NCI ethidium has been developed. To prove whether this test system allows to determine  $K_{app}$  values, we examined the capability of the well-characterized luminal NCI TPMP<sup>+</sup> to displace bound ethidium. The fluorescence spectrum of ethidium bound to nAChR shows an intensive emission at 590 nm upon excitation at 480 nm, when the agonist sites were saturated with the agonist carbachol [25]. Competitive displacement of bound ethidium by TPMP<sup>+</sup> could be directly determined by measuring the stepwise loss in fluorescence. Starting with a concentration of 100 nM TPMP<sup>+</sup> saturating concentrations of TPMP<sup>+</sup> were reached at 100  $\mu$ M, when bound ethidium was completely displaced by TPMP<sup>+</sup>. Using PhTX and poly(methylene tetramine) derivatives (Fig. 1) in back titration experiments comparable fluorescence spectra were obtained. Back titration of ethidium fluorescence with increasing concentrations of TPMP<sup>+</sup> is shown in Fig. 2A. Figure 2B shows representatively for all examined compounds the loss in fluorescence intensity obtained by addition of increasing concentrations of the PhTX analogue DCB-343. In all experiments basal fluorescence intensities were determined by completely displacing bound ethidium from the NCI site with 100  $\mu$ M TPMP<sup>+</sup> (Fig. 2B).

Binding affinities of various PhTX and poly(methylene tetramine) derivatives at concentrations ranging from 100 nM to 100  $\mu$ M were determined. Polyamines have been shown earlier to interact in millimolar concentrations with negatively charged phospholipid head groups [30]. As this interaction could influence the fluorescence of ethidium bound to nAChR by allosteric mechanisms, higher concentrations than 100  $\mu$ M have not been examined. Figure 3A–E shows the resulting dose–response curves, which were obtained by back titration of ethidium fluorescence and semilogarithmic plotting of the data. Applying the equation for the determination of dissociation constants described by Herz *et al.* [25]  $K_{app}$  values for the competing NCIs have been calculated from the semilogarithmic plots (Fig. 3F–K).

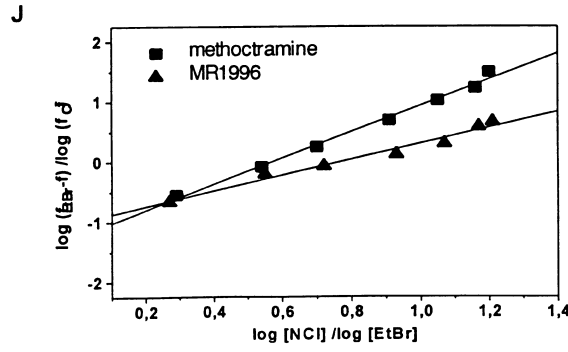
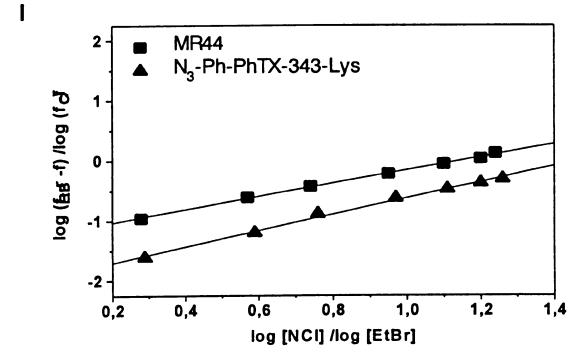
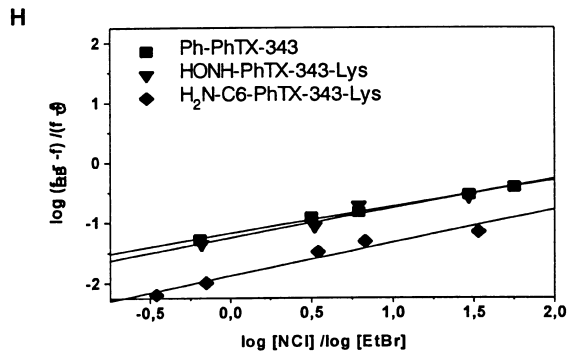
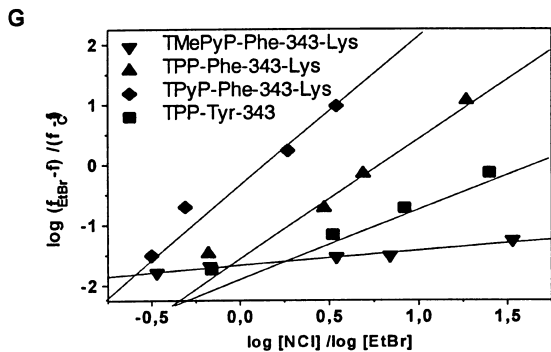
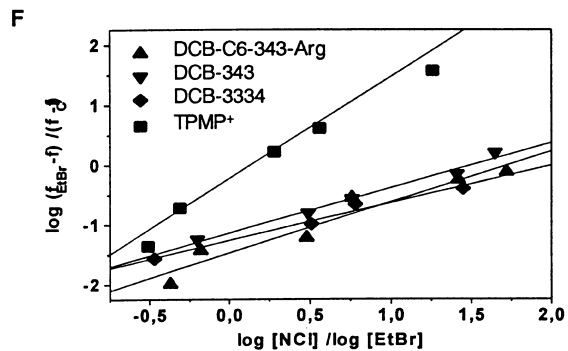
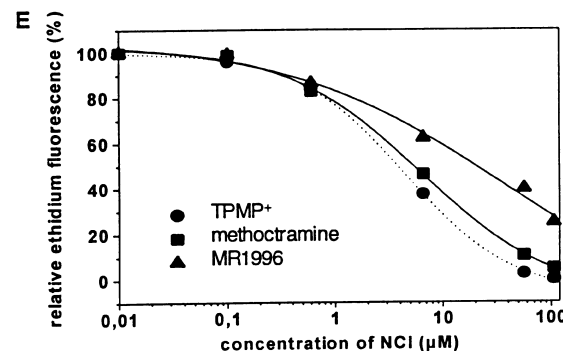
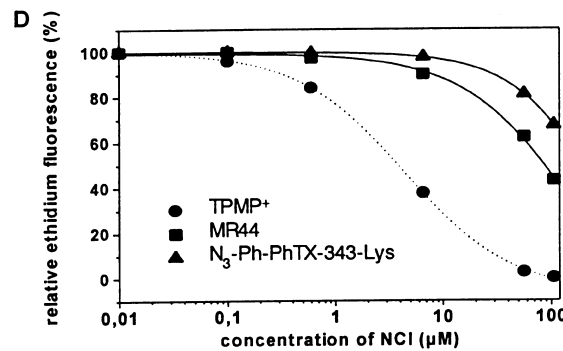
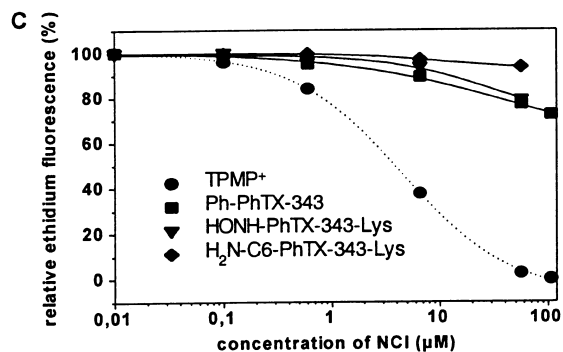
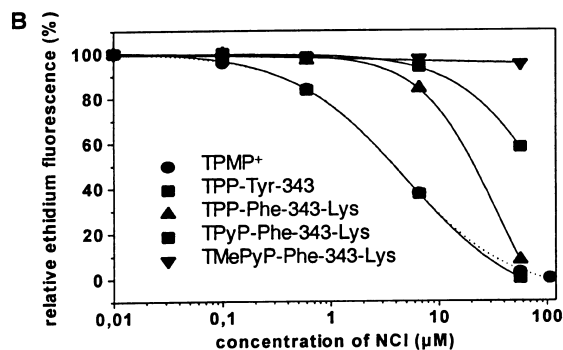
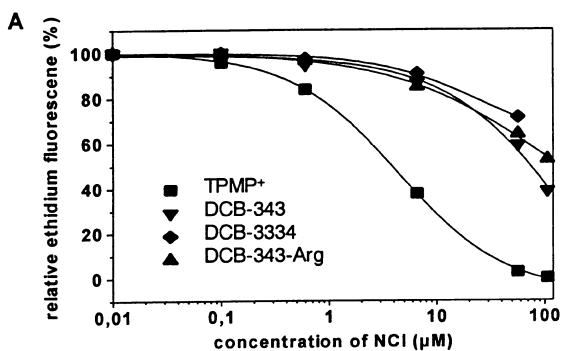
In the present study, three major classes of PhTX analogues have been examined, namely dihydrocarbamazepine derivatives, porphyrin PhTX derivatives, which carry extended aromatic ring systems and simple PhTX derivatives with 1–2 aromatic residues (Fig. 1). To identify compounds with improved binding affinities, the polyamine moiety of the PhTX derivatives has been chemically altered too. Furthermore, the symmetric poly(methylene tetramine) methoctramine, the asymmetric mono-methoctramine MR1996 and an azido derivative have been tested for their affinity to bind to the NCI site.

**Table 1.** IC<sub>50</sub> and  $K_{app}$  values of PhTX and poly(methylene tetramine) derivatives examined. ND (not determined) = IC<sub>50</sub> > 200  $\mu$ M or  $K_{app}$  > 1 mM.

Derivative	IC <sub>50</sub> ( $\mu$ M)	$K_{app}$ ( $\mu$ M)
Simple PhTX derivatives:		
Ph-PhTX-343	ND	114
HONH-PhTX-343-Lys	ND	87
H <sub>2</sub> N-C6-PhTX-343-Lys	ND	671
Dihydrocarbamazepine PhTX derivatives:		
DCB-343	75	8.1
DCB-3334	ND	26
DCB-C6–343-Arg	120	13
Porphyrin PhTX derivatives:		
TTP-Tyr-343	70	9.8
TPP-Phe-343-Lys	20	4.9
TPyP-Phe-343-Lys	3.5	0.3
TMePyP-Phe-343-Lys	ND	ND
Poly(methylene tetramine) derivatives:		
Methoctramine	4.2	0.9
MR1996	90	1.5
Azido polyamine derivatives:		
N <sub>3</sub> -Ph-PhTX-343-Lys	ND	7.3
MR44	80	3.5

Dihydrocarbamazepine PhTX derivatives have two planar ring systems, which have been flexibly connected to a third aromatic ring, forming the hydrophobic head group of these compounds (Fig. 1A). Within this group DCB-343 had the highest binding affinity with a  $K_{app}$  value of 8.1  $\mu$ M (Table 1). Elongation of the polyamine chain either by inserting an additional methylene amine, thereby also altering the relative distance between the positive charges, or by coupling  $\epsilon$ -amino-hexanoic acid or a terminal arginine both reduced the affinities of the DCB-PhTX analogues yielding  $K_{app}$  values of 26  $\mu$ M and 13  $\mu$ M, respectively (Table 1). The second class of PhTX derivatives carried a large planar porphyrin system, which was further extended by three flexibly connected aromatic side chains (Fig. 1B). These compounds bound very efficiently to the NCI site of the nAChR. Coupling an additional arginine residue in the polyamine chain and exchanging the tyrosine by a phenylalanine improved the binding properties twofold, as seen from the  $K_{app}$  values for TPP-Phe-343-Lys and TPP-Tyr-343 of 4.9  $\mu$ M and 9.8  $\mu$ M, respectively (Table 1). Replacing the four phenyl by three pyridyl residues, which were unprotonated under physiological conditions, resulted in a further increase in binding affinity. Interestingly, the introduction of three permanent positive charges by methylation of the N atoms of the pyridyl residues completely prevented binding to the NCI site. The hydrophobic properties of the third group of PhTX derivatives examined were less prominent, as these compounds contained only two simple aromatic residues and,

**Fig. 3.** Competitive dissociation of the ethidium-nAChR complex by various PhTX and poly methylene tetramine derivatives in presence of carbachol bound to the agonist binding site. Incremental amounts of the toxins were added to a solution containing nAChR membranes (1  $\mu$ M receptor concentration), ethidium (3  $\mu$ M in A–C; 6.5  $\mu$ M in D,F) and carbachol (1 mM). Measurements of ethidium fluorescence ( $\lambda_{ex}$  = 480 nm,  $\lambda_{em}$  = 590 nm) resulted in a titration profile, which was semilogarithmically plotted yielding concentration–response curves (A–E). Hill plots of the competitive dissociation of ethidium from nAChR membranes were calculated from the loss in ethidium fluorescence obtained by the toxins investigated in A–E. The data are plotted logarithmically where [NCI] and [EtBr] are concentrations of the competing toxin and ethidium, respectively.  $f_{EtBr}$  denotes the fluorescence in absence of competing toxins.  $f_{NCI}$  denotes the fluorescence when bound ethidium was completely displaced from the nAChR by TPMP<sup>+</sup> (100  $\mu$ M),  $f$  denotes the fluorescence observed at any given concentration of competing toxin during the back titration.



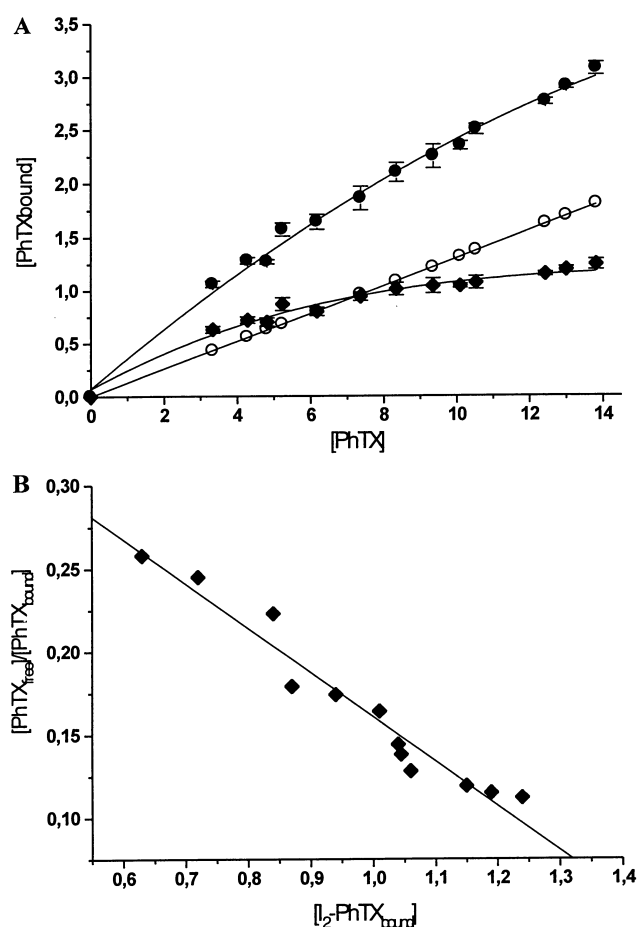


**Fig. 4.** Binding of  $N_3$ -Ph- $^{125}I_2$ -PhTX-343-Lys to the nAChR. (A) AChR-rich membranes ( $0.3 \text{ mg} \cdot \text{mL}^{-1}$  protein) were incubated with increasing concentrations of  $N_3$ -Ph- $^{125}I_2$ -PhTX-343-Lys ( $3$ – $14 \text{ } \mu\text{M}$ ). The specific binding ( $\blacklozenge$ ) of  $N_3$ -Ph- $^{125}I_2$ -PhTX-343-Lys was determined by subtracting the binding in presence of a 100-fold molar excess of  $N_3$ -Ph-PhTX-343-Lys ( $\circ$ ) from the total binding ( $\bullet$ ). Each value is the mean  $\pm$  SD of four separate experiments. (B) Scatchard plot of the binding of  $N_3$ -Ph- $^{125}I_2$ -PhTX-343-Lys to nAChR-rich membranes. The  $K_{\text{app}}$  value was  $3.7 \pm 0.3 \text{ } \mu\text{M}$  ( $r = 0.97$ ). Calculations based upon saturation of binding sites ( $1.6 \pm 0.3 \text{ } \mu\text{M}$ ) resulted in 1 mol of PhTX bound per 1 mol of  $\alpha$ -BTX binding site indicating a stoichiometry of 2 mol of PhTX per mol of receptor monomer.

in addition, in one derivative the phenyl group was replaced by a positively charged amino carbonic acid (Fig. 1C). For Ph-PhTX-343, which is structurally most similar to the natural occurring toxin PhTX-433, a surprisingly low binding affinity with a  $K_{\text{app}}$  value of  $114 \text{ } \mu\text{M}$  was observed (Table 1). Increasing the length of the polyamine chain by coupling the positively charged amino acid lysine and inserting a photolabile azido group into the aromatic ring of the phenyl residue significantly improved the potency (Fig. 1D), while the exchange of this moiety by a polar uncharged residue, such as the hydroxylamine group generated a 10-fold less active compound (Fig. 1C; Table 1).

Methoctramine, which carries at each end of its polyamine chain an aromatic moiety (Fig. 1E), competed efficiently with ethidium at the NCI site showing a  $K_{\text{app}}$  value of  $0.9 \text{ } \mu\text{M}$  (Table 1). Removal of one of the aromatic residues generates an asymmetric poly(methylene tetramine) derivative with reduced binding affinity. Inserting an azido group and altering the substituents at the aromatic ring lead to a further decrease in activity by a factor of two (Fig. 1D; Table 1).

Fixation of nAChR with glutardialdehyde in presence of desensitizing amounts of carbachol 'freezes' the receptor in its desensitized state [31]. Thereby, the receptor subunits are cross-linked to each other, which leads to a more rigid structure and prevents allosteric transitions. After treatment of nAChR with glutardialdehyde the fluorescence intensity of ethidium, when bound to the chemically fixed receptor, was reduced by 30–35%. However, the  $K_{\text{app}}$  for ethidium bound to this cross-linked receptor remained unchanged (data not shown). Fluorescence titration using the competing NCI TPMP<sup>+</sup> (Fig. 2C) to prove the binding properties of the fixed receptor resulted in a  $K_{\text{app}}$  for TPMP<sup>+</sup>, which was comparable to that found in the unfixed form (data not shown). Addition of DBC-343 in a concentration representing its  $\text{IC}_{50}$  value resulted in a 50% decrease in fluorescence intensity (Fig. 2D). Similar competition fluorescence spectra were obtained for the other NCIs examined (spectra not shown). The basal fluorescence was determined by adding  $100 \text{ } \mu\text{M}$  TPMP<sup>+</sup> for complete dissociation of bound ethidium from the NCI site.

The stoichiometry of high-affinity binding of PhTXs at the NCI site was determined using a radiolabeled PhTX derivative in a direct binding assay. Therefore  $N_3$ -Ph-PhTX-343-Lys was iodinated with  $^{125}I$  at one of its two aromatic rings. The reaction products were purified by RP-HPLC and the bi- $^{125}I$ -derivative was identified by MALDI-mass spectrometry. As shown in Fig. 4A total of PhTX binding could be resolved into a saturable binding component superimposed on a linear nonspecific component. Subtraction of the linear component, which was determined in presence of a 100-fold molar excess of the nonradioactive PhTX analogue, yielded saturable PhTX binding. A Scatchard plot of these data shown in Fig. 4B indicates that  $N_3$ -Ph- $^{125}I_2$ -PhTX-343-Lys binds to a single class of nonallosterically interacting binding sites with a  $K_{\text{app}}$  of  $3.7 \pm 0.3 \text{ } \mu\text{M}$ . PhTX binding reached saturating concentrations at  $1.6 \pm 0.3 \text{ } \mu\text{M}$ , from which  $5.3 \text{ pmol} \cdot \mu\text{g}^{-1}$  binding sites were calculated. As  $5.7 \text{ pmol} \cdot \mu\text{g}^{-1}$   $\alpha$ -BTX binding sites were determined, the number of PhTX binding sites appears equal to the number of  $\alpha$ -BTX binding sites. Binding of  $N_3$ -Ph- $^{125}I_2$ -PhTX-343-Lys in presence of the luminal NCIs TPMP<sup>+</sup> ( $150 \text{ } \mu\text{M}$ ) and tetracaine ( $300 \text{ } \mu\text{M}$ ) prevented specific binding of the PhTX derivative yielding linear nonspecific binding (data not shown).

For radiolabeling experiments  $N_3$ -Ph- $^{125}I_2$ -PhTX-343-Lys ( $10 \text{ } \mu\text{M}$ ;  $250\,000 \text{ c.p.m.} \cdot \text{nmol}^{-1}$ ) was incubated with nAChR-rich membranes ( $140 \text{ nM}$  receptor concentration) from *T. californica* and cross-linked to amino acid residues facing the ligand binding pocket by irradiation for 45 s at 254 nm. The  $^{125}I$ -labeled subunits of nAChR were separated by SDS/PAGE and visualized by autoradiography. All five receptor subunits were labeled, although with varying intensities. The two  $\alpha$ -, and

**Table 2.** Labeling yields obtained by photocross-linking of  $N_3$ -Ph- $^{125}I_2$ -PhTX-343-Lys to nAChR. The lanes shown in Fig. 5 of the dried gel were sliced and fractions were counted for radioactivity in a  $\gamma$ -counter. Labeling yields (in percentage of mol cross-linked PhTX per mol nAChR subunit) were calculated. Each value is the mean  $\pm$  SD of two separate experiments.

Subunit(s)	$\delta$	$\gamma$	$\beta$	$\alpha$
No addition	$7.5 \pm 0.2$	$4.2 \pm 0.4$	$11.1 \pm 0.4$	$10.6 \pm 0.6$
$500 \text{ } \mu\text{M}$ carbachol	$8.4 \pm 0.4$	$4.3 \pm 0.4$	$12.6 \pm 0.6$	$13.3 \pm 0.2$
$540 \text{ nM}$ $\alpha$ -BTX	$7.6 \pm 0.2$	$4.1 \pm 0.8$	$10.1 \pm 0.6$	$10.0 \pm 1.4$
$500 \text{ } \mu\text{M}$ TPMP <sup>+</sup>	$3.2 \pm 0.4$	$1.4 \pm 0.6$	$3.8 \pm 0.6$	$3.1 \pm 0.2$

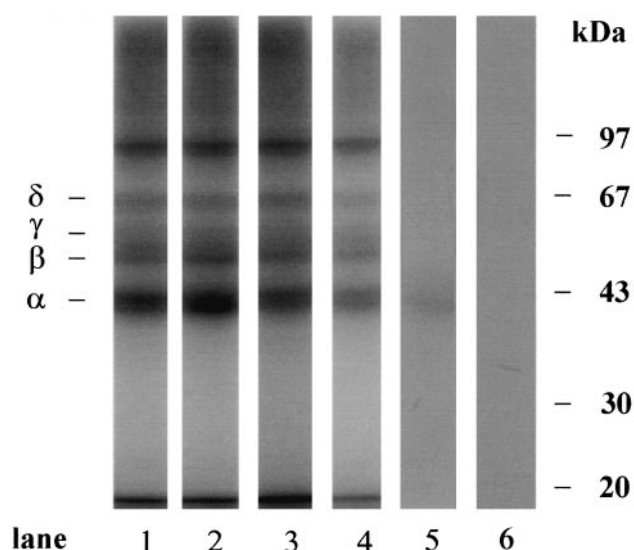


**Fig. 5. Photoaffinity labeling of nAChR with  $N_3$ -Ph- $^{125}I_2$ -PhTX-343-Lys.** nAChR-rich membranes were labeled with  $N_3$ -Ph- $^{125}I_2$ -PhTX-343-Lys and receptor subunits were separated using SDS/PAGE. Radioactive receptor subunits were visualized by autoradiography. nAChR-rich membranes (140 nM receptor concentration) were cross-linked with  $10 \mu\text{M}$   $N_3$ -Ph- $^{125}I_2$ -PhTX-343-Lys (lane 1) in the presence of  $500 \mu\text{M}$  carbachol (lane 2) or  $560 \text{ nM}$   $\alpha$ -BTX (lane 3) or  $500 \mu\text{M}$  TPMP<sup>+</sup> (lane 4) or  $1 \text{ mM}$   $N_3$ -Ph-PhTX-343-Lys (lane 5). Lane 6 containing  $10 \mu\text{M}$   $N_3$ -Ph- $^{125}I_2$ -PhTX-343-Lys bound to nAChR-rich membranes was not irradiated.

the  $\beta$ -,  $\gamma$ - and  $\delta$ -subunits were labeled with yields of 10.4%, 11.1%, 4.0% and 7.4%, respectively (Fig. 5, lane 1; Table 2). The presence of  $500 \mu\text{M}$  carbachol, which leads to receptor desensitization, resulted in an increase in total cross-linking intensity with the strongest effect on the  $\alpha$ - and  $\beta$ -subunit (Fig. 5, lane 2, Table 2). The competitive antagonist  $\alpha$ -BTX ( $540 \text{ nM}$ ) apparently did not affect binding of  $N_3$ -Ph- $^{125}I_2$ -PhTX-343-Lys (Fig. 5, lane 3, Table 2), while TPMP<sup>+</sup> caused a 65% decrease in labeling intensity in all receptor subunits (Fig. 5, lane 4). The specificity of binding was demonstrated by cross-linking  $N_3$ -Ph- $^{125}I_2$ -PhTX-343-Lys in the presence of a 100-fold molar excess of the nonradioactive analogue resulting in a decrease of the labeling yield to background levels (Fig. 5, lane 5). Without irradiation no cross-linking was observed (Fig. 5, lane 6). The  $\text{Na}^+$ - $\text{K}^+$ -ATPase, a 100-kDa protein, which is found as a contamination in nAChR-rich membrane preparations, was also radioactively labeled (Fig. 5). This observation does not disprove the specificity of the reaction as it has been shown that polyamines modulate activities of  $\text{Na}^+$ - $\text{K}^+$ -ATPase from different origins [32].

## DISCUSSION

Using the well-characterized luminal NCIs ethidium and TPMP<sup>+</sup> as reference the site and affinity of binding of a series of polyamines can be described. The aim of these experiments is the elucidation of the binding pocket for polyamines. The variation of the ligand's structural elements is a powerful tool to obtain information on the sterical and chemical properties of the binding pocket. With this information in hand more potent ligands can be developed. Finally the contributing receptor sequences have to be analyzed by photoaffinity-labeling.

We have utilized fluorescence titration to determine binding affinities of various PhTX and poly(methylene tetramine)

derivatives. The fluorescent NCI ethidium, when bound to the high-affinity NCI site on the nAChR in its desensitized state, shows an intensive emission maximum at  $590 \text{ nm}$  [25]. As bound ethidium was displaceable by well-characterized luminal NCIs, such as TPMP<sup>+</sup> and chlorpromazine, ethidium can be used as a reference fluorophor to characterize yet unknown NCIs competing for this binding site. The PhTXs and poly(methylene tetramine)s investigated in this study were found to compete with bound ethidium indicating that these compounds act also as luminal high-affinity NCIs. To exclude the possibility that the displacement of ethidium by polyamine derivatives is caused by an allosteric mechanism, the nAChR was fixed in its desensitized state by chemical cross-linking. Previous studies [31] demonstrated that covalent cross-linking of the receptor's neighboring subunits abolishes allosteric transitions by preventing structural flexibility. Ethidium bound to nAChR fixed in its desensitized state can still be displaced by the same TPMP<sup>+</sup> and chlorpromazine concentrations as used previously with unfixed receptor. Furthermore, polyamine derivatives competed with ethidium bound to covalently fixed nAChR in concentrations of their  $\text{IC}_{50}$  values leading to a decrease in fluorescence intensity to approximately 50%. These observations demonstrate that ethidium is removed at the NCI site by a competitive nonallosteric mechanism. Therefore, we and others [25] conclude that ethidium in micromolar concentrations is bound in the channel lumen. Ethidium binding to sites in the lipid annulus can be excluded, as ethidium has very low affinity to these binding sites and shows, when bound, no fluorescence at  $590 \text{ nm}$ . Therefore ethidium, PhTXs and poly(methylene tetramine)s most likely bind to the same binding site, namely the high-affinity NCI site of the nAChR.

In order to understand which structural elements of PhTXs and poly(methylene tetramine)s are important for high-affinity binding to nAChR, we varied the structure of these compounds to induce alterations in their binding affinities. Obvious trends in the  $K_{\text{app}}$  values have been observed: Increasing the size of the hydrophobic head group of the PhTXs by introducing a bulky aromatic ring system significantly improved the binding affinity for nAChR, when compared with Ph-PhTX-343, the compound most similar to the natural occurring toxin PhTX-433. Inserting a positively charged group or an uncharged hydroxylamine group into the hydrophobic head group largely reduced the binding affinity. Substituting the phenyl groups of TPP-Phe-343-Lys by pyrimidyl residues clearly improved the binding properties. Accordingly, the hydrophobicity of the head group of PhTX seems to represent an important structural element, which significantly contributes to high-affinity binding of these compounds. Therefore, the binding site of the PhTX's head group is supposed to be located in the hydrophobic upper part of the channel pore. This suggestion is compatible with the supposed hydrophobic character of the ethidium binding site with limited accessibility to the aqueous phase [25,33]. In comparison to DCB-343 the binding affinity of DCB-3334 was decreased threefold, demonstrating that the number of positive charges and their distribution within the polyamine chain modulates but not destroys the affinity. Furthermore, coupling of a terminal lysine residue improved the binding properties, whereas a terminal arginine residue slightly diminished them. Although, the positive charges are distributed at fixed lengths along the polyamine chain, the conformationally flexible carbon chain presumably still allows binding to the appropriate sites within the binding pocket. Due to the positive charges the polyamine chain is believed to interact with the negatively charged rings

located within the receptor's channel pore forming the selectivity filter [7,8]. Our observations on the binding affinities are in good agreement with earlier findings of Anis *et al.* [22] and Nakanishi *et al.* [23]. Additional to their data we are able to present  $K_{app}$  values for the various PhTX derivatives: constant values, which are independent from  $K_{app}$  values of the competing ligand used in the test system.

In comparison to PhTX derivatives the poly(methylene tetramine)s showed higher binding affinities. Methoctramine, a symmetric analogue known to act as antagonist on the muscarinic AChR [34], bound with high-affinity to the NCI site of the nAChR. Removing one of the terminal methoxybenzyl groups results in the asymmetric MR1996, resulted in a twofold reduced binding affinity. A photolabile poly(methylene tetramine) developed for photocross-linking experiments bound with slightly decreased affinity. Accordingly, one hydrophobic head group is sufficient for binding to the high-affinity NCI site on the nAChR. Furthermore, the long polyamine chain of these derivatives appeared to be advantageous for binding.

To ascertain that competition of PhTX derivatives with bound ethidium takes place at the high-affinity NCI site in the channel pore and to exclude the possibility that displacement of bound ethidium is allosterically caused by binding of PhTX derivatives to multiple, although low-affinity binding sites in the lipid annulus we have investigated the radiolabeled PhTX  $N_3$ -Ph- $^{125}I_2$ -PhTX-343-Lys in direct binding studies. The straight line obtained in the Scatchard plot indicates that this PhTX analogue binds to a single class of nonallosterically interacting binding sites. The stoichiometry of PhTX binding was determined to be 2 PhTX molecules/receptor monomer. Furthermore the well-characterized luminal NCIs TPMP<sup>+</sup> and tetracaine were found to completely dissociate specifically bound PhTX indicating that both PhTX binding sites are located in the channel lumen. Our findings demonstrate that two PhTX molecules bind with equal affinity with the channel lumen of nAChR. It is important to mention that recently Lu *et al.* [35] found evidence for the simultaneous binding of three polyamines in the inner pore of inwardly rectifying K<sup>+</sup> channels.

The radioactive photolabile  $N_3$ -Ph- $^{125}I_2$ -PhTX-343-Lys was further used in photocross-linking studies to explore the three-dimensional structure of the PhTX binding site. During UV-irradiation the azidophenyl group of this compound is able to covalently cross-link to any nearby amino acid facing the ligand binding site [36]. The observation that  $N_3$ -Ph- $^{125}I_2$ -PhTX-343-Lys photolabeled all five receptor subunits strongly suggests that the PhTX binding site is located deep within the channel, where the PhTX derivative is in close contact to all subunits. However, the labeling yields per subunit varied between 4.2% to 11.1% indicating that the hydrophobic head group of PhTX appeared to prefer defined sterical orientations upon binding. When preincubating nAChR-rich membranes with the agonist carbachol, which induces receptor desensitization accompanied with an increase in binding affinity for NCIs, we observed a clear enhancement in the labeling intensity. Cross-linking in presence of TPMP<sup>+</sup> demonstrated that 65% of the bound PhTX analogue was displaceable. Consequently, during irradiation this compound seems to cross-link to additional binding sites on the nAChR, possibly the low-affinity binding sites in the lipid annulus [37].

Electrophysiological studies have shown that spermine [19] and PhTX-343 [20] have multiple sites of action on muscle nAChR, similar to those observed for ionotropic glutamate receptors [16]. From binding studies Choi *et al.* [26] suggested

that PhTX analogues act on the nAChR's ionic channel in its open conformation. Our findings demonstrate that the photolabile PhTX derivative binds to nAChR also in absence of agonist with the receptor being predominantly in its resting closed channel state. Furthermore, when nAChR was preincubated with carbachol, which rapidly shifted the vast majority of nAChR to the desensitized closed channel state, the PhTX analogue was cross-linked with even higher affinity. The PhTX binding site must therefore be accessible in the open and the closed channel conformation. Results obtained by applying the substituted cysteine accessibility method [38] showed that a number of low molecular mass reagents were able to react in the closed channel state with a number of M2 cysteine substitution mutants, including  $\alpha$ T244C close to the intracellular end of the channel. Furthermore, using the same technique Wilson and Karlin [39] could recently localize the narrowest part of the ion channel between  $\alpha$ G240C and  $\alpha$ T244C, a region which includes the negatively charged cytosolic ring of the selectivity filter. In the closed state a barrier in this narrow part of the channel was detected restricting the accessibility for small reagents from both sides of the ion channel [39]. Choi *et al.* [26] assumed that PhTX is orientated toward the cytoplasmic side of the pore. Although the authors tried to label the open channel conformation, addition of carbachol as performed in their studies presumably resulted in rapid desensitization and channel closure rather than in channel opening. Because in the closed state molecules cannot pass the channel pore, PhTX bound from the cytosolic side would not be able to compete with ethidium for binding at the high-affinity NCI site, which is known to be located in the extracellular part of the ion channel [13]. Based on our results that PhTXs and poly(methylene tetramine)s displace ethidium bound at the high-affinity NCI site in the channel's closed conformation we conclude that polyamine derivatives are orientated toward the extracellular side of the ion channel. Furthermore, we could demonstrate that 2 PhTX molecules bind with equal affinity in the channel lumen. Consequently, the most likely mode of binding which leads to receptor inhibition is that the PhTX derivatives enter from the extracellular side of the receptor's ionic channel. The hydrophobic head groups are believed to bind in the hydrophobic upper part of the channel pore to the high-affinity NCI site, while the positively charged polyamine chains most likely interact with the negatively charged selectivity filter located deep within the channel pore. Experiments to prove this localization by photoaffinity labeling and microsequencing of the labeled receptor peptides are underway. Furthermore, it would be most interesting to extend these studies on neuronal nAChRs, however, an expression system providing the amount of receptor necessary for this work would have first to be established.

Our results on the modification of polyamine binding affinities by altering their structural elements and our photoaffinity approach provide important information on the molecular structure of the binding site of polyamine derivatives at the nAChR. This model possesses optimized properties in terms of charge distribution, size and hydrophobic interactions providing the structural data required for the rational design of novel, more potent polyamine derivatives selectively inhibiting the nAChR.

## ACKNOWLEDGEMENTS

This work was supported by the European Commission, BIOMED-2 program contract BMH4-CT97-2395 (to F. H.), Fond der Chemischen Industrie (to F. H.) and NIH grant AI 10187 (to K. N.). We would like to

thank Prof. A. Herrmann (Institut für Biophysik, Humboldt-Universität Berlin) for kindly allowing us to use of Aminco Bowman spectrometer. We also thank H. Bayer for helpful technical assistance and Dr X. Huang (Columbia University, New York, USA) for kindly supplying porphyrin PhTX analogues.

## REFERENCES

- Changeux, J.-P. (1990) Functional architecture and dynamics of the nicotinic acetylcholine receptor: an allosteric ligand-gated ion channel. *Fidia Res. Found. Neurosci. Award Lect.* **4**, 21–168.
- Karlin, A. & Akabas, M.H. (1995) Towards a structural basis for the function of nicotinic acetylcholine receptors and their cousins. *Neuron* **15**, 1231–1244.
- Hucho, F., Tsetlin, V. & Machold, J. (1996) The emerging three-dimensional structure of a receptor, the nicotinic acetylcholine receptor. *Eur. J. Biochem.* **239**, 539–557.
- Noda, M., Takahashi, H., Tanabe, T., Toyosato, M., Kikuyotani, S., Furutani, Y., Hirose, T., Takashima, H., Inayama, S., Miyata, T. & Numa, S. (1983) Structural homology of *Torpedo californica* acetylcholine receptor subunits. *Nature* **302**, 538–532.
- Hucho, F., Oberthür, W. & Lottspeich, F. (1986) The ion channel of the nicotinic acetylcholine receptor is formed by the homologous helices M II of the receptor subunits. *FEBS Lett.* **205**, 137–142.
- Galzi, J.-L., Devillers-Thiéry, A.Q., Hussy, N., Bertrand, S., Changeux, J.-P. & Bertrand, D. (1992) Mutations in the ion channel domain of a neuronal nicotinic acetylcholine receptor convert ion selectivity from cation to anionic. *Nature* **359**, 500–505.
- Imoto, K., Busch, C., Sakmann, B., Mishina, M., Konno, T., Nakai, J., Bujo, H., Mori, Y., Fukudo, K. & Numa, S. (1988) Rings of negatively charged amino acids determine the acetylcholine receptor channel conductance. *Nature* **335**, 645–648.
- Konno, T., Busch, C., Von Kitzing, E., Imoto, K., Wang, F., Nakai, J., Mishina, M., Numa, S. & Sakmann, B. (1991) Rings of anionic amino acids as structural determinants of ion selectivity in the acetylcholine receptor channel. *Proc. R. Soc. Lond. B Biol. Sci.* **244**, 69–79.
- Blount, P. & Merlie, J.P. (1989) Molecular basis of the two nonequivalent ligand binding sites of the muscle nicotinic acetylcholine receptor. *Neuron* **3**, 349–357.
- Pedersen, S.E. & Cohen, J.B. (1990) d-Tubocurarin binding sites are located at  $\alpha$ - $\delta$  and  $\alpha$ - $\gamma$  subunit interfaces of the nicotinic acetylcholine receptor. *Proc. Natl Acad. Sci. USA* **87**, 2785–2789.
- Giraudat, J., Dennis, M., Heidmann, T., Chang, J.Y. & Changeux, J.-P. (1986) Structure of the high-affinity binding site for noncompetitive blockers of the acetylcholine receptor: serine 262 of the delta subunits is labeled by  $^3\text{H}$ -chlorpromazine. *Proc. Natl Acad. Sci. USA* **83**, 2719–27213.
- Arias, H.R. (1998) Binding sites of exogenous and endogenous non-competitive inhibitors of the nicotinic acetylcholine receptor. *Biochem. Biophys. Acta* **1376**, 173–220.
- Hucho, F. & Hilgenfeld, R. (1989) The selectivity filter of a ligand-gated ion channel. The helix-M2 model of the ion channel of the nicotinic acetylcholine receptor. *FEBS Lett.* **257**, 17–23.
- Adams, M.E., Carney, R.L., Enderlin, F.E., Fu, E.T., Jarema, M.A., Li, J.P., Miller, C.A., Schooley, D.A., Shapiro, M.J. & Venema, V.J. (1987) Structure and biological activities of three synaptic antagonists. *Biochem. Biophys. Res. Comm.* **148**, 678–683.
- Eldefrawi, A.T., Eldefrawi, M.E., Konno, K., Mansour, N.A., Nakanishi, K., Oltz, E. & Usherwood, P.N.R. (1988) Structure and synthesis of a potent glutamate receptor antagonist in wasp venom. *Proc. Natl Acad. Sci. USA* **85**, 4910–4913.
- Usherwood, P.N.R. & Blagbrough, I.R. (1991) Spider toxins affecting glutamate receptors: polyamines in therapeutic neurochemistry. *Pharmacol. Therap.* **52**, 245–268.
- Ragsdale, D., Gant, D.B., Anis, N.A., Eldefrawi, A.T., Eldefrawi, M.E., Konno, K. & Miledi, R. (1989) Inhibition of rat glutamate receptors by philanthotoxin. *J. Pharmacol. Exp. Ther.* **251**, 156–156.
- Rozental, R., Scoble, G.T., Albuquerque, E.X., Idriss, M., Sherby, S., Sattelle, D.R., Nakanishi, K., Konno, K., Eldefrawi, A.T. & Eldefrawi, M.E. (1989) Allosteric inhibition of nicotinic acetylcholine receptors of vertebrates and insects by philanthotoxin. *J. Pharmacol. Exp. Ther.* **349**, 123–130.
- Shao, Z., Mellor, I.S., Brieley, M.J., Harris, J. & Usherwood, P.N.R. (1998) Potentiation and inhibition of nicotinic acetylcholine receptors by spermine in the TE671 human muscle cell clone. *J. Pharmacol. Exp. Ther.* **286**, 1269–1276.
- Jayaraman, V., Usherwood, P.N.R. & Hess, G.P. (1998) Inhibition of the nicotinic acetylcholine receptor by philanthotoxin-343; kinetic investigations in the microsecond time region using laser-pulse photolysis technique. *Biochemistry* **38**, 11406–11414.
- Scott, R.H., Sutton, K.G. & Dolphin, A.C. (1993) Interactions of polyamines with neuronal ion channels. *Trends Neurosci.* **16**, 153–160.
- Anis, N., Sherby, S., Goodnow, R., Niwa, M., Konno, K., Kallimopoulos, T., Bukownik, R., Nakanishi, K., Usherwood, P., Eldefrawi, A. & Eldefrawi, M. (1995) Structure-activity relationships of philanthotoxin analogs and polyamines on N-methyl-D-aspartate and nicotinic acetylcholine receptors. *J. Pharmacol. Exp. Ther.* **254**, 764–773.
- Nakanishi, K., Huang, X., Jiang, H., Liu, Y., Fang, K., Huang, D., Choi, S.-K., Katz, E. & Eldefrawi, M. (1997) Structure-binding relation of philanthotoxins from nicotinic acetylcholine receptor binding assay. *Bioorg. Med. Chem.* **5**, 1969–1988.
- Schiebler, W., Lauffer, L. & Hucho, F. (1977) Acetylcholine receptor enriched membranes: acetylcholine binding and excitability after reduction *in vivo*. *FEBS Lett.* **81**, 39–41.
- Herz, J.M., Johnson, D.A. & Taylor, P. (1987) Interaction of noncompetitive inhibitors with the acetylcholine receptor. *J. Biol. Chem.* **262**, 7238–7247.
- Choi, S.-K., Kalivretenos, A.G., Usherwood, P.N.R. & Nakanishi, K. (1995) Labeling studies of photolabile philanthotoxins with nicotinic acetylcholine receptors: mode of interaction between toxin and receptor. *Chem. Biol.* **2**, 23–32.
- Greenwood, F.C., Hinter, W.M. & Glover, J.S. (1963) The preparation of  $^{131}\text{I}$ -labelled human growth hormone of high specific radioactivity. *Biochem. J.* **89**, 114–121.
- Hartig, P.R. & Raftery, M.A. (1979) Preparation of right-side-out, acetylcholine receptor enriching intact vesicles from *Torpedo californica* electroplaque membranes. *Biochemistry* **18**, 1146–1150.
- Laemmli, U.K. (1970) Cleavage of structural proteins during assembly of head of bacteriophage T4. *Nature* **227**, 680–685.
- Chung, L., Kaloyanides, G., McDaniel, R., McLaughlin, A. & McLaughlin, S. (1985) Interaction of gentamicin and spermine with bilayer membranes containing negatively charged phospholipids. *Biochemistry* **24**, 442–452.
- Watty, A., Methfessel, C. & Hucho, F. (1997) Fixation of allosteric states of the nicotinic acetylcholine receptor by chemical cross-linking. *Proc. Natl Acad. Sci. USA* **94**, 8202–8707.
- Heinrich-Hirsch, B., Ahlers, J. & Peter, H.W. (1977) Inhibition of Na,K-ATPase from chick brain by polyamines. *Enzyme* **22**, 235–241.
- Herz, J.M. & Atherton, S.J. (1992) Steric factors limit access to the noncompetitive inhibitor site of the nicotinic acetylcholine receptor. *Biophys. J.* **62**, 74–76.
- Melchiorre, C. (1990) Polymethylene tetramines: a novel class of cardioselective M2 antagonists. *Med. Chem. Rev.* **10**, 327–349.
- Lu, T., Nguyen, B., Zhang, X. & Yang, J. (1999) Architecture of a  $\text{K}^+$  channel inner pore revealed by stoichiometric covalent modification. *Neuron* **22**, 571–580.
- Henriksen, U. & Buchardt, O. (1990) Aryl azides as photolables. Retention of iodine during photochemical ring expansion of an iodinated tyrosine derivative. *Tetrahedron Lett.* **31**, 2443–2444.
- Heidmann, T., Oswald, R.E. & Changeux, J.-P. (1983) Multiple sites of

- action for noncompetitive blockers on acetylcholine receptor rich membrane fragments from *Torpedo marmorata*. *Biochemistry* **22**, 3112–3127.
38. Akabas, M.H., Kaufmann, C., Archdeacon, P. & Karlin, A. (1994) Identification of acetylcholine receptor channel-lining residues in the entire M2 segment of the  $\alpha$  subunit. *Neuron* **13**, 919–927.
39. Wilson, G.G. & Karlin, A. (1998) The location of the gate in the acetylcholine receptor channel. *Neuron* **20**, 1269–1281.